THE ATMOSPHERIC HEAT SOURCE OVER THE BOLIVIAN PLATEAU FOR A MEAN JANUARY

GANDIKOTA V. RAO
Department of Earth and Atmospheric Sciences, Saint Louis University
Saint Louis, Missouri 63108, U.S.A
SUAT ERDOGAN
Devlet Meteoroloji İşleri Genel Müdürlüğü . Kalaba / ANKARA

Abstract. The atmospheric heat sources of large plateaus strongly influence the general circulation particularly in the summer season. The Bolivian plateau and the adjacent areas affect the upper tropospheric flow in a typical summer month by developing an anticyclone and deflecting the prevailing westerlies. The plateau initially warms the atmosphere through sensible heating and then through latent heating as thunderstorms develop.

The atmospheric heat source over the Bolivian and adjacent plateau was computed employing conventional surface and satellite radiation data for the mean January 1979. Because of a lack of direct ground temperature data, the surface radiation was estimated following an empirical formula devised for some earlier Tibetan studies.

The results revealed that the latent heating developing in the eastern and northeastern part of the plateau is the biggest contributor to the atmospheric heat source (500 W m^{-2}). A comparison of these results against similar recent results from Tibet showed that the atmospheric heat source in South America is stronger than that over Tibet, primarily because of increased rainfall over Bolivia.

1. Introduction

The elevated plateaus of Bolivia and Tibet are known to influence the atmospheric circulation in their general vicinity in several ways (Schwerdtfeger, 1961; Flohn, 1968). Their influence is particularly strong in the summer season when the pleateaus are sensibly heated (differentially with respect to the adjacent air). This sensible heating draws moist air from the low levels near the plateau, setting off thunderstorms. The latent heat released in the thunderstorms further warms the atmosphere over the plateau. An anticyclone then develops due to thermal winds in the upper levels in response to this total heating. The intensity of the anticyclonic circulation is thus dependent on the heat source over the plateau and an estimation of the heat source is thus vital to understand the dynamics of the circulation.

Gutman and Schwerdtfeger (1965) made a tentative surface energy budget over the Altiplano using data from EL Alto La Paz, Oruro and La Quiaca to determine the role of latent and sensible heat in the development of a high pressure system over the subtropical Andes in summer. Figure 1 shows these and other stations, whose names and locations are given which are also listed in Appendix A. Virji (1981) verified the existence of an upper level anticyclonic circulation over Bolivia using NOAA/GOES satellite cloud-tracked winds. He estimated the center of the anticyclone to be at 17° S, 65° W. Another climatological study based on about 20 years of upper air data was presented by Rao and

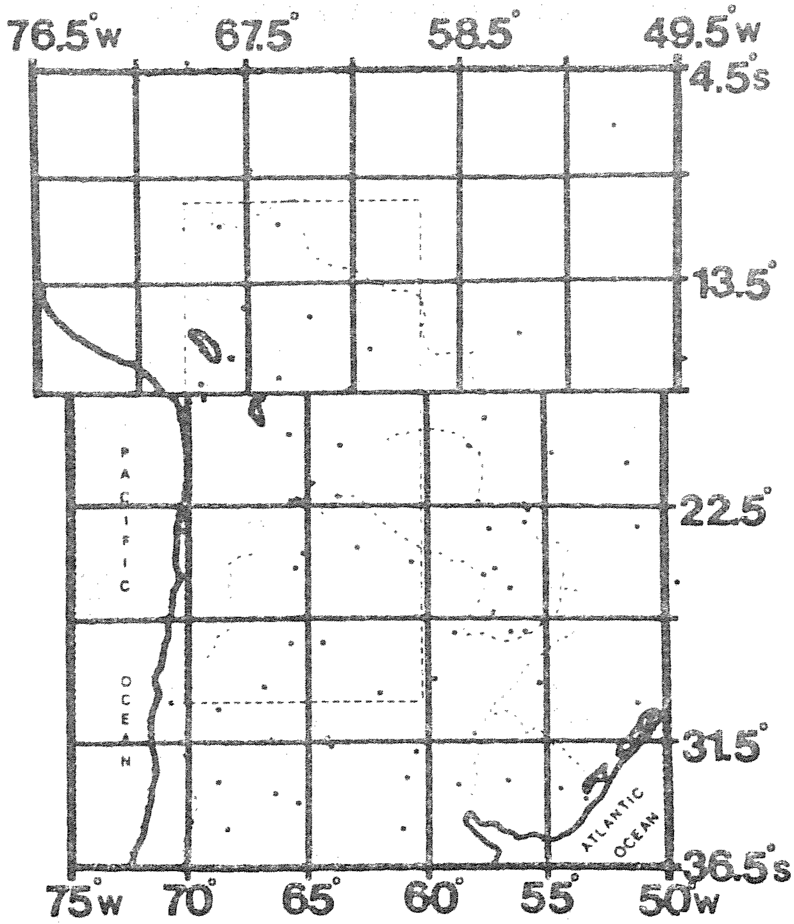

Fig. 1. Dots indicate surface stations. Squares: target areas for which Nimbus-7 ERB data were available. Area enclosed by dashed line is the area of interest.

van de Boogaard (1986). Figure 2 shows the mean January 200 mb streamlines and isotachs from an atlas by van de Boogaard *et al.* (1989). It is clear that westerlies dominate tropical South America except where the Bolivian anticyclone develops. The center of this anticlone is at 16° S, 67° W, agreeing well with the Virji's (1981) location. It is noteworthy that some easterlies develop to

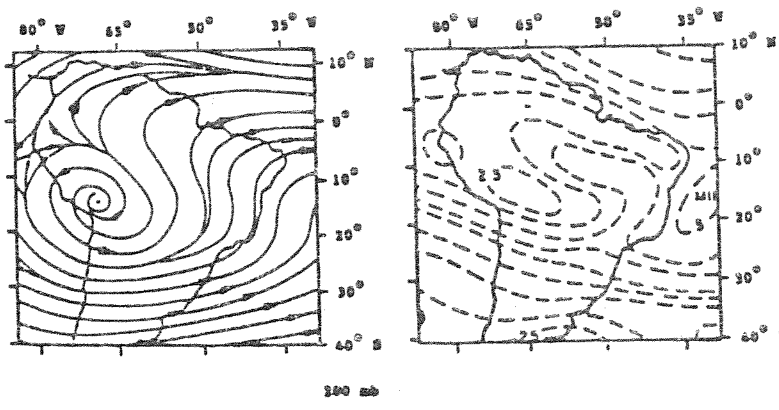

Fig. 2. Streamlines and isotachs (m s^{-1}) at 200 mb (from Rao and van de Boogaard, 1986). Notice the development of the anticyclone over Bolivia and adjacent plateau and the resulting easterlies to the north.

the north of this high pressure area. These easterlies are not particularly strong because the prevailing winds are westerlies. Evidently this anticyclone is seasonally controlled and belongs to the realm of upper monsoons.

The main objectives of this research are:

(a) to estimate preliminarily the sensible, latent and radiative heat fluxes over the Bolivian and adjacent plateau, and to compare their relative magnitudes and,

(b) to define the locations of the centers of the sensible, latent and radiative heat sources for January 1979.

2. Data and Analysis of Validation

The Andes are formed by two primary chains of mountains joined in several places by ridges or spurs which separate the basins. From central Peru southward these basins tend to be at higher altitudes, reaching a maximum in the huge Altiplano of the Bolivian plateau which has a flat basin of some 100 000 km^2 at an average altitude of 3800 m. Using conventional surface and satellite data, the integrated value of the heat source over the Altiplano area has been estimated for January 1979. This month appears to be representative of a non-El Nino summer, and 1979 was a FGGE year when additional conventional and satellite observations were available. During El Nino years, precipitation and convective activity are typically below normal.

Data from a wide area extending from 5° S to 35° S and 50° W to 75° W have been analyzed. Although the heat source calculation took place in that broad area, emphasis was placed on the area enclosed by 10° S and 30° S and 60° W and 70° W. The Altiplano occupies only a portion of this area.

(a) Elevation of surface stations

The elevation of each surface station was obtained from the Monthly Climatic Data for the World (MCDW) (see U.S. Department of Commerce (1979a)) or from Gates and Nelson (1973).

(b) Surface air temperature (T_a)

January 1979 mean T_a's (shelter air temperatures) were available from 31 stations (see Appendix A for a listing and Figure 1 for an indication of network density). The data were obtained from the MCDW. The manner of deducing the atmospheric mean quantities varies from country to country, as was discussed by Schwerdtfeger (1976). It is assumed that similar practices are being continued.

(c) Surface pressure

The 1979 January mean surface pressure data were obtained for the stations in

Appendix A from the MCDW. For the calculation of drag coefficients which are dependent on elevation, mean station pressure was used.

(d) WATER VAPOR PRESSURE

To estimate the contribution of long-wave radiation from water vapor to surface net radiation, water vapor pressure was needed. These data were obtained for the stations in Appendix A from the MCDW.

(e) WIND SPEED

Wind speed affects sensible heat flux. The January climatological wind speed data were obtained from the World Survey of Climatology (Schwerdtfeger, 1976). The number of stations in the vicinity of the boxed area in Figure 1 is sixteen. The data covered different periods, the average periods being about 10 years. See Appendix A for a listing of the stations. Data from the boxed area and its vicinity were utilized in the analysis.

(f) PRECIPITATION

January 1979 average rainfall was obtained for the 31 stations from the MCDW. Latent heat released in precipitation was calculated from these rainfall estimates. Over the Altiplano, high pressure area, precipitation amounts were observed (e.g., Santa Cruz reported an average of 601 mm of rain).

(g) HOURS SUNSHINE

The January climatological number of hours of sunshine for each station was used for the calculation of a cloudiness index. These data for seven stations (see Appendix A) in the boxed area in Figure 1 were obtained from the World Survey of Climatology (Schwerdtfeger, 1976). Additional data were interpolated from the World Maps of Climatology (Landsberg *et al.*, 1963). The data for January 1979 compared favorably with long-term climatological values.

(h) NIMBUS-7 DATA

Nimbus 7 is sun-synchronous polar orbiting satellite at 955 km with local noon ascending node and midnight descending node of equatorial crossing. The satellite carried an Earth Radiation Budget (ERB) radiometer that measured simultaneously the incoming solar radiation, outgoing earth-reflected (shortwave) and emitted (longwave) radiation. The Nimbus-7 ERB radiometer provided both Wide Field of View (WFOV) and Narrow Field Of View (NFOV) measurements. Thw WFOV measurements represent outgoing flux at the satellite level. The NFOV measurements represent intensity of radiance at a specific angle.

There are some differences between ERB NFOV and WFOV global net radiation results over a one-year period. Both ERB NFOV and WFOV data were mapped onto a world grid of 2070 target areas. The target area assigned to any measurement was based upon the location of the center of the field of view

TABLE I

The mean value of 38 target areas of Nimbus-7 ERB NFOV and WFOV albedo (α_p) and net radiation (R_∞) for January 1979. These 38 target areas are shown in Figure 1.

	NIMBUS-7	
	Albedo (%)	R_∞ Net radiation (W m^{-2})
NFOV	36.10	86.21
WFOV	30.13	91.29
NFOV-WFOV	5.97	−5.08

(FOV). The size of the FOV depends upon the scan angle with respect to the satellite nadir axis, but the linear dimension of the FOV is always <150 km (smaller than the target areas). The FOV subtends a cap of the earth with an earth central angle of almost 60° of plane angle for WFOV measurements. Therefore, WFOV measurements cover over 14 latitude zones. However, more than half of the measured flux comes from the central four or five latitude zones. Because of the effective resolution, NFOV data are more realistic than WFOV data for small areas.

In this research, 38 Nimbus-7 ERB targets were used for January 1979. These targets are evenly distributed in time over that month. The mean value of these targets was calculated for each ERB NFOV and WFOV measurement of net radiation and planetary albedo. Table I shows that WFOV net radiation exceeded NFOV net radiation by ~5.08 W m^{-2}. Furthermore the NFOV albedo (a_p) exceeded the WFOV albedo by ~5.97%. These differences are small compared to the annual differences (Arking and Vemury, 1984). No correction was made for the NFOV net radiation (R_∞) and albedo (α_p) values used.

(i) TIROS-N DATA

The sun-synchronous TIROS-N satellite is located at an average altitude of 854 km. The orbital period is about 101.6 min. TIROS-N has the Advanced Very High Resolution Radiometer (AVHRR) instrument. Visible imageries of a total of 25 days of January 1979 were obtained from the Environmental Satellite Imagery (U.S. Department of Commerce, 1979b). Each target area measuring 5° by 5° was divided into four subtargets; and cloudiness was then estimated over these subtargets and converted to a percentage.

3. Computational Method

The atmospheric heat source over the Bolivian plateau was estimated in a manner similar to that of Chen *et al.* (1985).

The vertical integral of the apparent heat source which is denoted by $\langle Q1 \rangle$ determines radiative and turbulent flux divergence for the whole atmospheric thickness. It can be written as

$$\langle Q1 \rangle = \frac{1}{g} \int_{P_t}^{P_s} Q1 \, dp \approx \frac{1}{g} \int_{P_t}^{P_s} Q1_R \, dp + \mathrm{LE} + \mathrm{SH}, \tag{1}$$

where P_s and P_t are the surface pressure and pressure at the top of the atmosphere, respectively; LE is the net latent heat flux, SH the sensible heat flux, the term $\langle Q1 \rangle$ is called the atmospheric heat source and the term $Q1_R$ denotes the radiative flux divergence. Only the radiative flux divergence values for sufficiently deep atmospheric layers can be found with some accuracy (Kondratyev, 1972). In this research, the atmosphere is divided into two layers: (1) troposphere, surface to 200 mb and (2) an upper layer encompassing stratosphere and mesosphere. We can combine the radiative flux divergence for the two layers as:

$$\frac{1}{g} \int_{P_t}^{P_s} Q1_R \, dp = \frac{1}{g} \int_{P_t}^{200\,\mathrm{mb}} Q1_R \, dp + \frac{1}{g} \int_{200\,\mathrm{mb}}^{P_s} Q1_R \, dp. \tag{2}$$

We are primarily interested in the radiative flux divergence between the surface and 200 mb. Because there are no measurements of net radiative flux divergence between 200 mb and satellite level and because it is known that the radiative heating does not vary much in the upper layer, we ignored the net radiative flux divergence above the troposphere (represented by the first term on the right-hand side of Equation (2)) and let the NIMBUS-7 ERB NFOV measured R_∞ represent the net radiation at 200 mb.

It is further assumed that

$$R = (R_\infty - R_s) \approx \frac{1}{g} \int_{200\,\mathrm{mb}}^{P_s} Q1_R \, dp, \tag{3}$$

where R_s is surface net radiation. Both R_∞ and R_s are defined as positive if directed downward.

Nitta (1983) and Luo and Yanai (1984) calculated the values of $Q1$ (see Equation 4) at individual pressure levels and then performed a vertical integration for the Tibetan plateau. In our research, $Q1$ is computed directly from the balance equation:

$$\langle Q_1 \rangle = (R_\infty - R_s) + \mathrm{LE} + \mathrm{SH}, \tag{4}$$

where R_∞ (net radiation at the top of atmosphere) is obtained from Nimbus 7 ERB NFOV matrix tapes. Surface net radiation R_s is estimated from the following equation:

TABLE II

Empirical coefficients (A, B, a, b and c) in Equation 5. See Figures 3 and 4 and Table III for the significance of vegetation index.

Vegetation index	A	B	a	b	c
L, S	0.285	0.535	0.548	0.164	0.0220
C, P, N	0.121	0.612	0.548	0.164	0.0220
O	0.121	0.612	0.631	0.200	0.0084
2, 9, F	0.334	0.546	0.631	0.200	0.0084
1, 3	0.164	0.615	0.631	0.200	0.0084

$$R_s = S_0(A + BH/H_0)(1 - \alpha) - \delta\sigma[Tg^4 - Ta^4(a + bN + cE)]. \qquad (5)$$

In the above, S_0 is the solar radiation received at the top of the atmosphere. The coefficients A, B, a, b, c are listed in Table II. As may be inferred from Tables II and III, these coefficients, empirically determined in a field experiment over Tibet, are sensitive to vegetation cover. Figures 3 and 4 and Table III (Matthews, 1983) show the types of surface vegetation of the Tibetan and Bolivian plateaus, respectively. Based on type of vegetation, the Tibetan plateau can be categorized into four regions: (1) the northwestern Tibetan plateau is a desert; (2) the northeastern part has xeromorphic and dwarf shrubland, tall/medium/short grassland and meadow-type of vegetation; (3) the southeastern part is covered with tropical/subtropical evergreen seasonal broad-leaved and needle-leaved forest; and (4) the vegetation of the southwestern part of the Tibetan plateau gradually changes from desert to tropical/subtropical drought-deciduous and evergreen seasonal broad-leaved forest.

TABLE III

A brief explanation of the vegetation index shown in Figures 3 and 4.

Map symbol	Description
1	Tropical evergreen rainforest, mangrove forest.
2	Tropical/subtropical evergreen seasonal broadleaved forest.
3	Subtropical evergreen rainforest.
7	Tropical/subtropical evergreen needleleaved forest.
9	Evergreen broadleaved woodland.
C	Xeromorphic forest/woodland.
F	Tropical/subtropical drought-deciduaous forest.
L	Xeromorphic shrubland/dwarf shrubland.
N	Tall/medium/short grassland with 10–40% woody tree cover.
O	Tall/medium/short grassland with <10% woody tree cover or tuft-plant cover.
P	Tall/medium/short grassland with shrub cover.
R	Medium grassland, no woody cover.
S	Meadow, short grassland, no woody cover.
-	Desert.

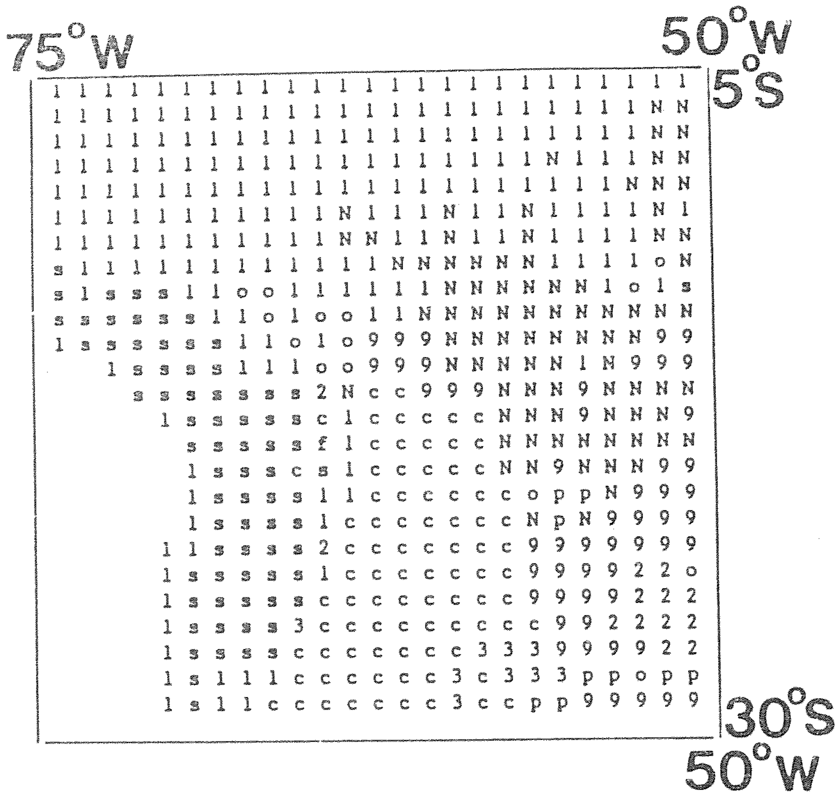

Fig. 3. Land-cover map of the Bolivian and adjacent plateau showing detailed subdivisions of major ecosystems. (Refer to Table III for explanation of symbols, from Matthews, 1983.)

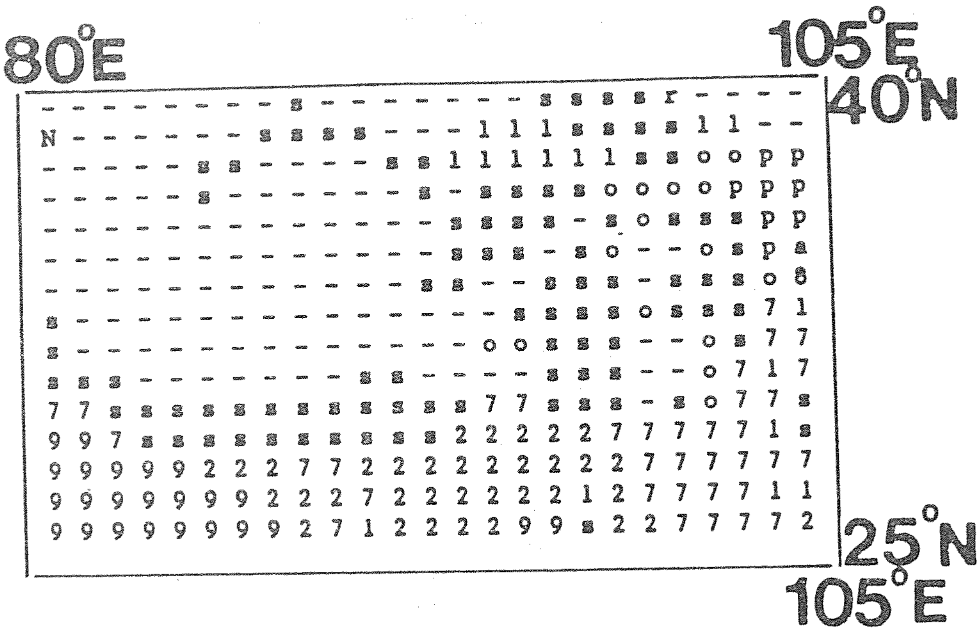

Fig. 4. Land-cover map of the Tibetan and adjacent plateau showing detailed subdivisions of major ecosystems. (Refer to Table III for explanation of symbols, from Matthews, 1983.)

The vegetation of the Bolivian plateau may also be categorized into four regions: (1) the northwestern part is covered with tropical evergreen rain and mangrove forest; (2) the northeastern plateau has tall/medium/short grassland with 10–40% woody tree cover; (3) the southeastern part is covered with xeromorphic/forest land; and (4) the southwestern plateau is covered with short grassland, meadow, short grassland and no woody cover.

In Equation 5, H is the observed solar radiation at the earth's surface. The maximum possible numbers of hours of insolation, H_0 (unit kJ m^{-2} h^{-1}) is given by Iqbal (1983):

$$H_0 = (24/\pi) I_{sc} E_0 \sin\phi \sin\delta[(\pi/180)\omega_s - \tan\omega_s], \qquad (6)$$

where I_{sc} is the solar constant expressed in energy units as 4871 kJ m^{-2} h^{-1}, ϕ latitude, δ the declination angle, E_0 the earth's eccentricity correction factor and ω_s the hour angle. These latter quantities were estimated in the usual ways from astronomical tables; see also Spencer (1971).

Observed insolation, H, was not available over the Bolivian plateau. To overcome this problem, the insolation-sunshine correlation (also called the cloudiness index) was used to estimate H/H_0. The monthly average daily radiation incident on a horizontal surface may be estimated using the number of hours of bright sunshine. The insolation-sunshine correlation of Glover and McCulloch (1958) was used;

$$H/H_0 = 0.29 \cos\phi + 0.52\bar{n}/\bar{N}_d \quad \text{for } \phi < 60°, \qquad (7)$$

where $\bar{n}$ is the monthly averaged observed hours of bright sunshine per day and $\bar{N}_d$ is the average daylength which may be obtained from astronomical tables.

Resuming the discussion of Equation 5, α is the surface albedo; $\delta = 0.95$ is the coefficient of emissivity; $\sigma = 5.6697 \times 10^{-8}$ (W m^{-2} K^{-4}) is the Stefan–Boltzman constant; N is cloud amount (expressed as a percentage) taken from TIROS-N satellite imageries (U.S. Department of Commerce 1979b); E is water vapor pressure (mb); T_a is shelter air temperature. T_g is ground temperature. A most difficult problem is estimating the ground temperature since such measurements do not exist in the public domain. The ground temperatures of the Bolivian plateau were extrapolated using data from other regions of the world of similar environments. Specifically, there appears to be some similarity in the types of surface vegetation and elevation between the Tibetan and the Bolivian plateaus. The regression line connecting T_g and T_a was obtained in the following manner:

Air temperatures (T_a) were obtained from the Monthly Climatic Data for the World (July 1979) for 6 Tibetan stations (see Appendix B). The ground temperature data of the Tibetan plateau were extrapolated from the July 1979 sensible heating and radiative cooling map of the Tibetan plateau (Chen *et al.*, 1985). July 1979 data were selected to obtain the regression equation because Nimbus 7 ERB NFOV net radiation (R_∞) and albedo (α_p) values were available for that month and Chen *et al.*'s (1985) Tibetan data also existed.

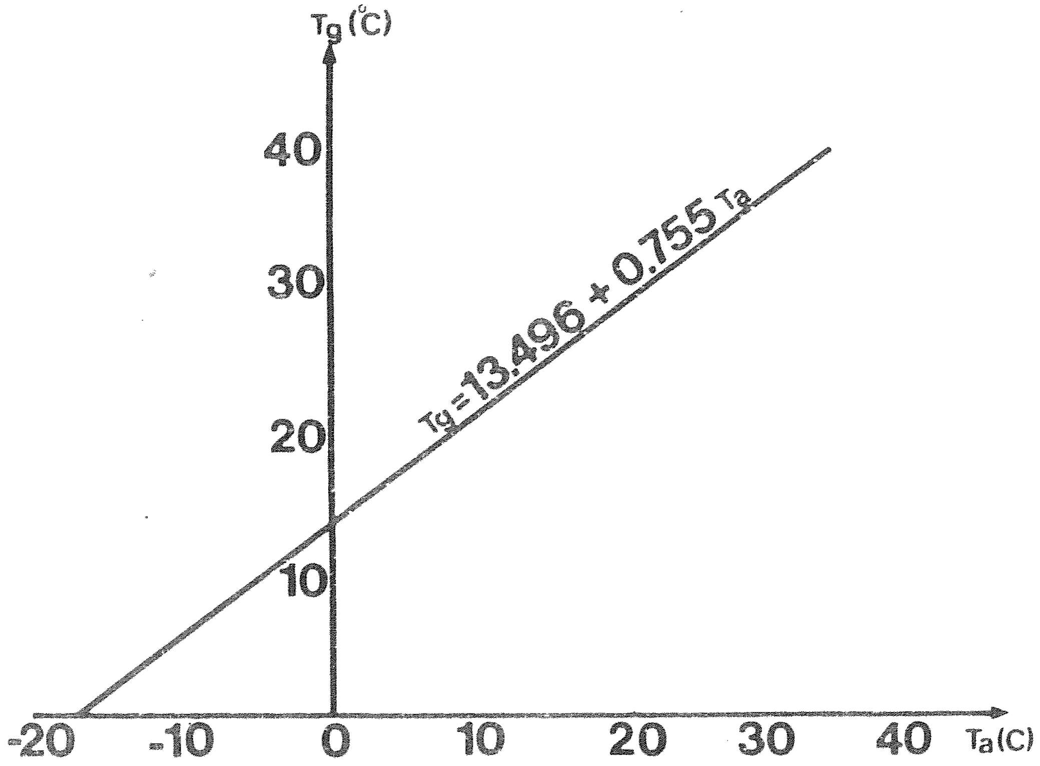

Fig. 5. Regression line between T_g and T_a based on the Tibetan station data for July 1979.

The regression equation between ground and air temperatures for July 1979 for the Tibetan plateau was found to be:

$$T_g = 13.496 + 0.755 T_a \,. \tag{8}$$

This regression (Figure 5) was applied to the Bolivian plateau to infer T_g in places where the surface vegetation was nearly the same as that in the Tibetan plateau, e.g., El Alto's mean January 1979 temperature was nearly 8 °C, and T_g was inferred to be 19.5 °C; as air temperature increased, the $(T_g - T_a)$ value decreased a little. As another example, Oruro's T_a for January 1979 was 17 °C; the corresponding T_g was computed to be 26 °C. Only through direct measurements would we be able to say that these estimates are reasonable. However, annual mean climatological $(T_g - T_a)$ data exist for certain stations in Argentina. Schwerdtfeger (1976) gives for Guemes (24° 36′ S, 64° 59′ W elevation 655 m) an average annual value of 2.9 °C, the summer values being higher. Our inferred range also appeared to be within the limits shown by Smith and Reiter (1986) for the Gobi desert.

The latent heat flux, LE, is given by

$$\text{LE} = 2.508 \times 10^6 \text{ (in mm of monthly rain at a surface station)}/31 \times 86400 \tag{9}$$

where L is given in W m^{-2}.

The sensible heat flux between ground and atmosphere is estimated from the aerodynamic formula:

$$SH = pC_pC_dV_0(T_g - T_a)\,, \tag{10}$$

where the air density, ρ, at the surface was obtained from the equation of state; C_p specific heat at constant pressure; v_0 (m s^{-1}), the wind speed at anemometer height and c_d the drag coefficient. While drag coefficients appropriate to gentle terrain (1.5–2.0×10^{-3}) are widely used, drag coefficients appropriate to high terrain are somewhat uncertain. Cressman (1960) suggested a value of 8.0×10^{-3} for high mountains and plateaus. New evidence (Chen *et al.*, 1985) suggests the following formula:

$$\begin{aligned} C_d &= 0.00112 + 0.01/V_0 && \text{for } z > 2800\text{ m.} \\ C_d &= 0.00112 + 0.01/V_0 - 0.00362(P_0 - 720)/280 && \text{for } Z < 2800\text{ m.} \end{aligned} \tag{11}$$

where Z is surface elevation and P_0 the surface pressure of a station. The new C_d values are smaller than Cressman's (1960) but Chen *et al.* (1985) found them to be realistic.

4. Results

(a) Latent heat, LE

Based on the monthly (January 1979) precipitation data, estimated latent heat flux (LE) released is shown in Figure 6. Over the northern and mid-eastern parts of the plateau, high LE values (200–300 W m^{-2} with maximum 562 W m^{-2}) are evident. The western, southern and southeastern parts of plateau have low LE values. These represent 2–3 °C/day heating rates for a 700–100 mb air column.

(b) Sensible heating, SH

Figure 7 shows isopleths of sensible heat flux. Over the mid-western plateau the average sensible heat flux is about 100 W m^{-2}. The equivalent heating rate is around 1 °C/day. Ground–air temperature differences varied from 6 to 13 °C over the plateau.

(c) Surface net radiation, R_s

The spatial and temporal variation of net radiation flux at the earth's surface (R_s) controls the redistribution of the available energy. Figure 8 shows isopleths of R_s. In the middle and northern parts of the plateau, the estimated flux is around 200–300 W m^{-2}. The highest surface net radiation, found over the western and southern parts of the plateau (400–500 W m^{-2}), appears to be due to high insolation and low albedo. In the same general area, high SH's are estimated

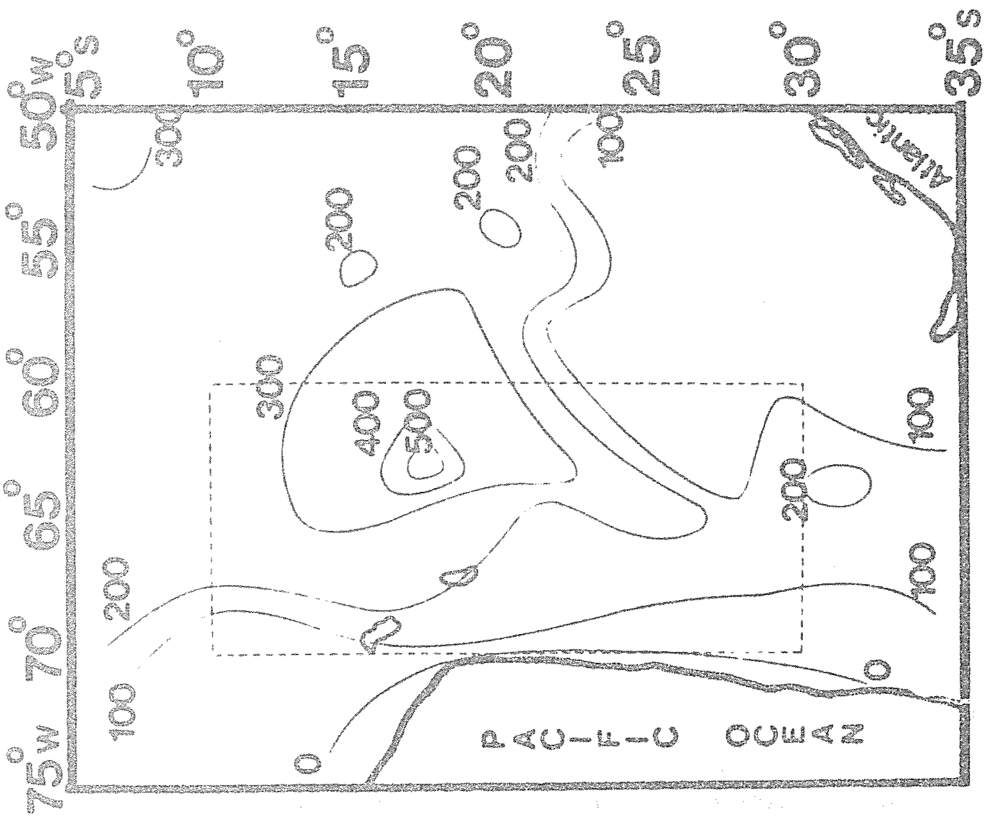

Fig. 6. Latent heat released in precipitation (LE) ($W m^{-2}$) over the Bolivian plateau and adjacent area during January 1979.

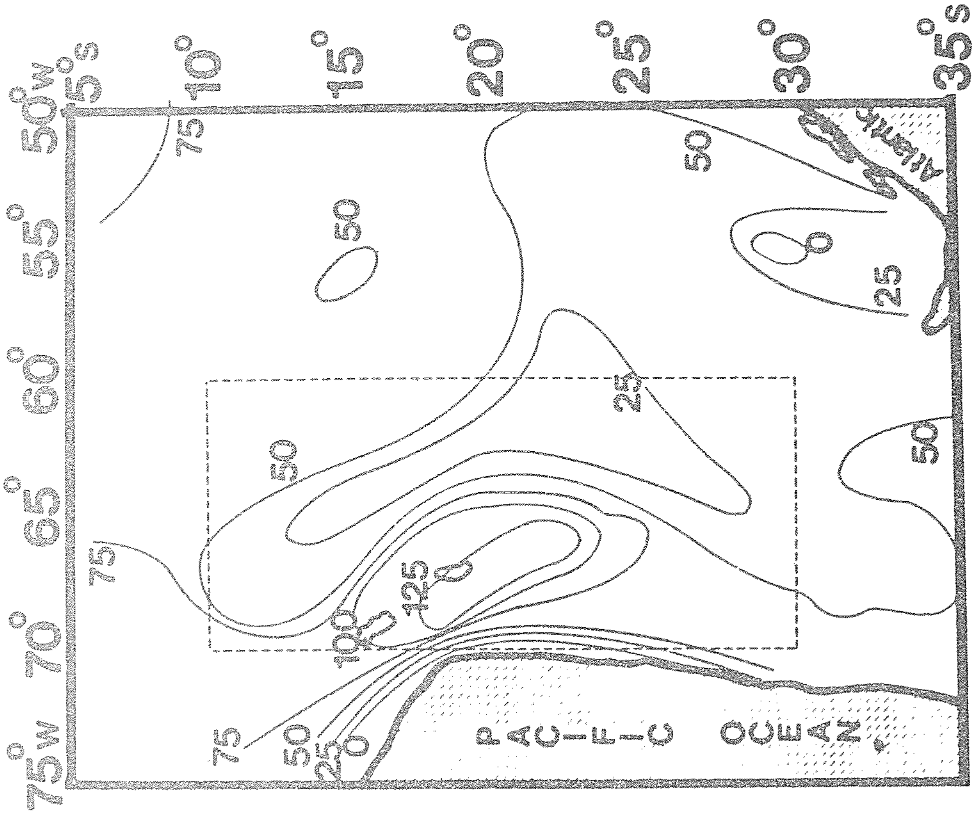

Fig. 7. Sensible heat flux (SH) ($W m^{-2}$) over the Bolivian plateau and adjacent area during January 1979.

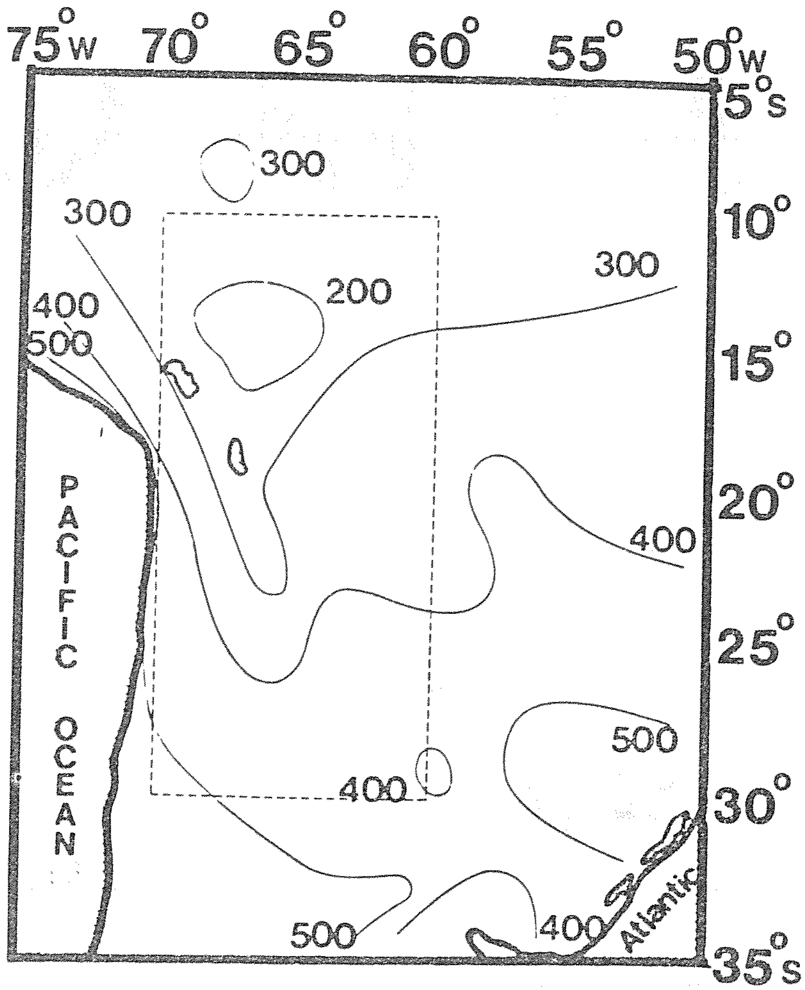

Fig. 8. Surface net radiation (R_s) (W m^{-2}) over the Bolivian plateau and adjacent area during January 1979.

because of large ($T_g - T_a$) differences. Surface net radiation (R_s) contributes to the heat source negatively (see Equation 3).

(d) Radiative cooling, R

Radiative cooling (R) was estimated by subtracting R_s from the radiation, R_∞, at the top of atmosphere (see Equation 3). Figure 9 shows that the smallest radiative cooling (115.3 W m^{-2}) occurred over the northwestern part of the plateau. The corresponding cooling rate for a 700–100 mb air column was −1 °C/day over the northern part, but −2 °C/day over the central plateau.

(e) Atmospheric heat source, $\langle Q1 \rangle$

Figure 10 shows the heat source $\langle Q1 \rangle$. The northern, eastern and middle parts of the plateau have positive fluxes implying diabatic heating, with the reverse situation in the southwestern and southeastern portions. Corresponding heating and cooling rates are shown in Figure 11 for a 700–100 mb air column. Over the northern and northeastern parts of the plateau, these rates range from 1 to

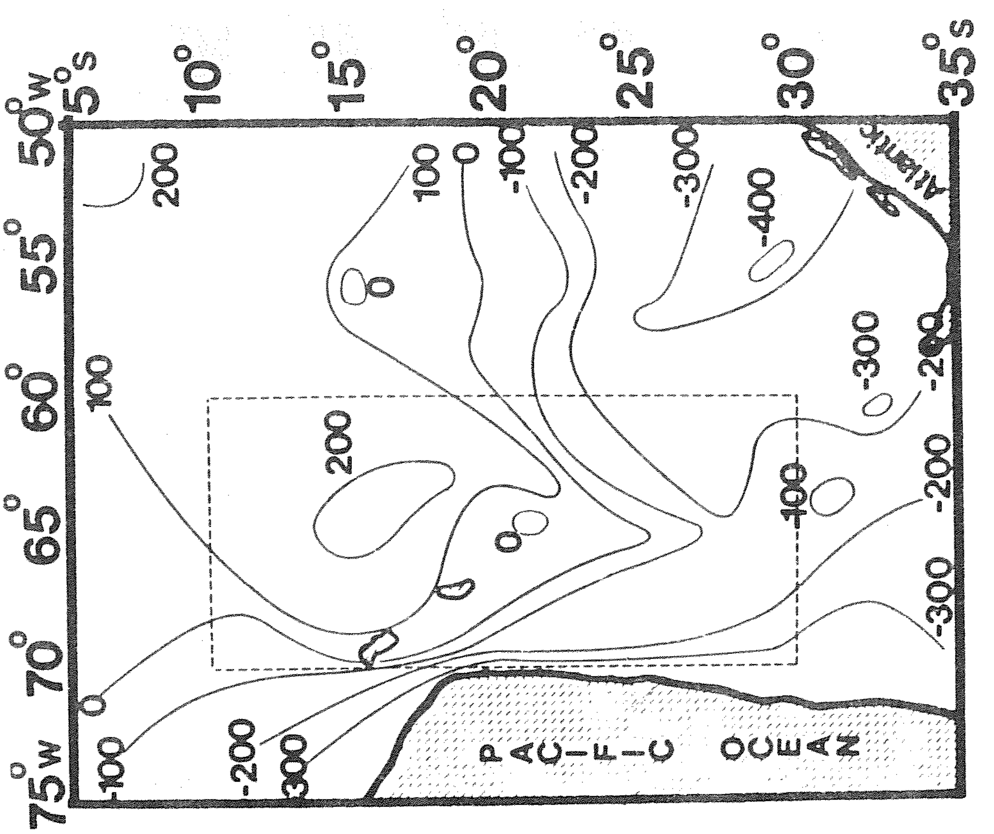

Fig. 10. Atmospheric heat source (sink) ($\langle Q1 \rangle$) in W m^{-2}) over the Bolivian plateau and adjacent area during January 1979.

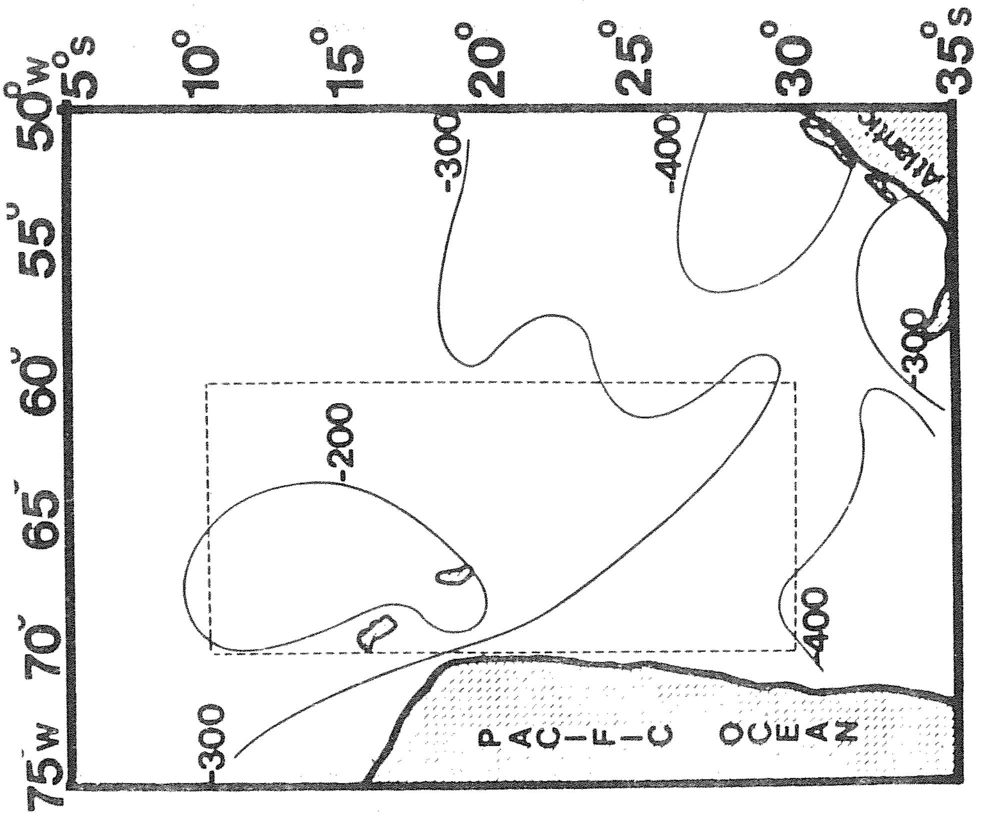

Fig. 9. Radiative cooling (R) (W m^{-2}) over the Bolivian plateau and adjacent area during January 1979.

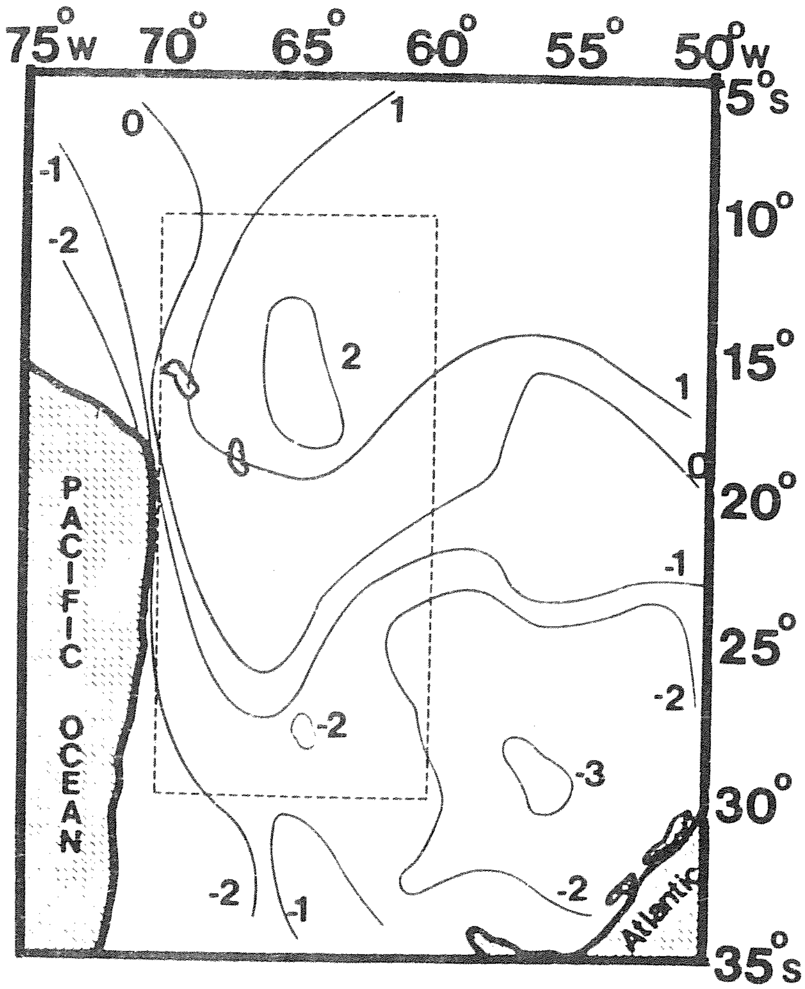

Fig. 11. Heating (cooling) rates of the heat source (sink) (degree/day).

2 °C/day, in the middle section from 0 to 1 °C/day and over the southern part from 0 to −2 °C/day.

In summary, it was found that latent heating dominates the northern and mid-eastern part of Altiplano, while sensible heating is most important in the western part. The atmospheric heat source over the northern, eastern and middle parts of the Altiplano contributes to the formation of the Bolivian upper anticyclone.

5. Comparison with Previous Results

Gutman and Schwerdtfeger (1965, hereafter GS) deduced an upper anticyclonic circulation over the Bolivian plateau based on data from one rawinsonde station (Antofagasta). Using surface data from La Paz, Oruro and La Quiaca, GS also estimated the heat budget for La Quiaca (22° 06′ S; 65° 36′ W at 3460 m). Table IV compares some of our results with theirs. The largest differences were found in the surface net radiation and sensible heat flux. La Quiaca is located on the southwestern part of Altiplano where the sensible heat flux was 126.2 W m^{-2} during January 1979 (due primarily to the high ground-air temperature

TABLE IV

Comparison of our results with those from Gutman and Schwerdtfeger (1965) for La Quiaca (22° 06′ S, 65° 36′ W).

	Gutman and Schwerdtfeger's (1965)	Our's	Difference
Albedo %	0.37	0.42	−0.5
Net radiation at the top of atmosphere W m^{-2}	43.58	81.88	−38.20
Net radiation at the surface W m^{-2}	184.01	291.68	−107.67
Latent heat precipitation W m^{-2}	116.2	123.6	−7.4
Sensible heating W m^{-2}	58.1	126.2	−68.1
Radiative cooling W m^{-2}	−140	−209.8	64.9
Vertical integrated heat flux W m^{-2}	48.42	40.04	8.38

differences. GS's sensible heat flux and surface net radiation were comparatively small because of their low climatological temperature differences and insolation values. Another difference is in the radiative cooling fluxes. GS estimated net radiation at the top of the atmosphere with a mathematical model, while we used data from Nimbus-7. The vertically integrated heat fluxes, however, are close to each other because the differences between sensible heat flux and surface net radiation are nearly the same.

Although our computation of R_S over the Bolivian plateau appears reasonable, direct measurement of this quantity is desirable. A measurement program similar to that of Sheaffer and Reiter (1987) is being discussed with scientists in Argentina.

6. Brief Comparison Between the Bolivian and Tibetan Plateau Heat Sources

The effects of the Tibetan plateau as a heat source in the general circulation has been recognized by many scientists (Staff Members Academia Sinica, 1958; Chen *et al.*, 1965; Yeh and Gao, 1979; Yeh and Chang, 1974). Classic monsoon theory postulates that heating of the Tibetan plateau contributes to the establishment of an upper anticyclone. Flohn (1968) concluded that the Tibetan summer anticyclone and the tropical easterly jet stream are caused by sensible heating of the high plateau and latent heating to the southeast of the Tibetan plateau. General circulation model studies (e.g., Hahn and Manabe, 1975), numerical model studies (Krishnamurti *et al.*, 1973; Luo and Yanai, 1983, 1984; Zheng and Liou, 1986; Kuo and Qian, 1981, 1982) and heat source studies of Nitta (1983), Reiter and Gao (1982), Chen *et al.* (1985) and Shen *et al.* (1986) indicate the intensity of the heat source. Similar studies have not yet been undertaken in the Bolivian plateau.

A comparison of conditions over the Tibetan and Bolivian plateaus is possible for the first time here because of the similarity in methodology and data reduction procedures between Chen *et al.* (1985) and the current study. Table V shows the heat sources and fluxes over the Bolivian and Tibetan plateaus. Precipitation was below normal in the 1979 monsoon over India and amounts over the Tibetan plateau were less than over the Bolivian plateau. An LE value of 80–140 W m^{-2} occurred in the eastern and southeastern parts of the Tibetan plateau. The western and southwestern parts of the Tibetan plateau displayed large values of sensible heat flux (80–100 W m^{-2}). The total heat source of the Tibetan plateau was greatest over the southeastern part of the plateau (80–120 W m^{-2}).

It appears that for both plateaus, sensible heat flux initiates convection, latent heat becoming dominant eventually. While for the western and southwestern parts of the Tibetan plateau, the sensible heat flux is most important, in the western and mid-western parts of the Bolivian plateau, the sensible heat flux is dominant. In the eastern part of the Tibetan plateau the latent heat flux is the major factor while in the eastern and northeastern portions of the Bolivian plateau, the latent heat flux is dominant. Radiative cooling appears to be more intense over the Bolivian plateau than over Tibet. The Tibetan heat source $Q1$ is most developed over the eastern and middle parts of the plateau (see Chen *et al.*,

TABLE V

Comparison of components of the heat budget of the Bolivian and Tibetan Plateaus with respect to their summers.

	Bolivian Plateau (January 1979)	Tibetan Plateau (July 1979)
Precipitation	Eastern and northeastern part (400–600) mm/month	Eastern part (150–200) mm/month
Sensible heat flux	Midwestern part (75–125) W m^{-2}	Western and southwestern part (80–110) W m^{-2}
Radiative cooling	Northwestern part of plateau 200 W m^{-2}	Southern part of plateau 110 W m^{-2}
Vertical integrated heat flux	Northeastern part of plateau (100–200) W m^{-2}	Mid and eastern part of plateau (100–120) W m^{-2}

1985) while the Bolivian plateau heat source is largest over the middle and northeastern parts of the Altiplano (Figure 10).

Acknowledgements

We would like to thank the Director of the National Space Science Data Center for supplying the NIMBUS-7 data; the Director of Institute of Physics, University of Bolivia; the Director of Hydrology, Chile; and the Director of the National Electricity Company, Santiago, Chile for providing additional data. We also thank Drs A. J. Pallmann and Carol Belt of Saint Louis University for their constructive comments. Eric Huag of Saint Louis University helped us with the reading of data and Juanita Ryles typed the manuscript.

Suat Erdogen wishes to thank the Ministry of Education, Government of Turkey for a scholarship and a travel award and his wife Burcin, for her encouragement. Dr G. V. Rao wishes to acknowledge the receipt of a Beaumont Faculty Development award which partly enabled him to do this research.

Appendix A

Station listing: p, pressure (mb), T, air temperature (°C), V, vapor pressure (mb), R, rain (mm) total for the month, and S79 sunshine expressed as percentage of long term average – all for January 1979, Ws, wind speed (m s^{-1}) from long-term climatological January values.

Stations	Latitude	Longitude	Elevation, m	Data
Arica/Chacalluta	18° 22′ S	70° 21′ W	35	*P*, *T*, *V*, *R* and Ws
Antofagasta/Cerro Moreno	23° 28′ S	70° 26′ W	122	*P*, *T*, *V*, *R* and Ws
La Serena	29° 54′ S	71° 15′ W	32	*P*, *T*, *V*, *R* and Ws
La Quiaca Observatorio	22° 06′ S	65° 36′ W	3459	*P*, *T*, *V*, *R*, Ws and S79
Jujuy Aero	24° 23′ S	65° 05′ W	905	*P*, *T*, *V*, and *R*
Salta Aero	24° 51′ S	65° 29′ W	1226	*P*, *T*, *V*, *R*, Ws and S79
Tucuman Aero	26° 50′ S	65° 12′ W	420	*P*, *T*, *V*, *R*, and Ws
Catamarca Aero	28° 36′ S	65° 46′ W	456	*P*, *T*, *V*, *R*, and Ws
La Rioja Aero	29° 23′ S	66° 49′ W	430	*P*, *T*, *V*, *R*, and S79
Jachal	30° 15′ S	68° 45′ W	1165	*P*, *T*, *V*, and *R*
Cordoba Aero	31° 19′ S	64° 13′ W	474	*P*, *T*, *V*, *R*, and Ws
Rivadavia	24° 10′ S	62° 54′ W	205	*P*, *T*, *V*, and *R*
Las Lomitas	24° 42′ S	60° 35′ W	130	*P*, *T*, *V*, *R*, and Ws
Santiago Del Estero Aero	27° 46′ S	64° 18′ W	199	*P*, *T*, *V*, *R*, Ws and S79
Pena	26° 49′ S	60° 27′ W	92	*P*, *T*, *V*, *R*, Ws and S79
Corrientes Aero	27° 27′ S	58° 46′ W	62	*P*, *T*, *V*, *R*, and Ws
Reconquista Aero	29° 11′ S	59° 40′ W	49	*P*, *T*, *V*, *R*, and S79
Ceres	29° 53′ S	61° 57′ W	88	*P*, *T*, *V*, *R*, Ws and S79
Cobija	11° 04′ S	68° 44′ W	260	*P*, *T*, *V*, and *R*
Riberalta	11° 00′ S	66° 05′ W	172	*P*, *T*, *V*, and *R*
Rurrenabaque	14° 28′ S	67° 35′ W	200	*P*, *T*, *V*, and *R*

Appendix A. (*Contd.*)

Trinidad	14° 45′ S	64° 48′ W	236	*P*, *T*, *V*, and *R*
Charana	17° 36′ S	69° 28′ W	4059	*P*, *T*, *V*, and *R*
Santa Cruz	17° 47′ S	63° 10′ W	437	*P*, *T*, *V*, and *R*
Camiri	20° 06′ S	63° 33′ W	792	*P*, *T*, *V*, and *R*
Tarija	21° 32′ S	64° 47′ W	1905	*P*, *T*, *V*, and *R*
Yacuiba	22° 01′ S	63° 43′ W	580	*P*, *T*, *V*, *R*, and Ws
El Alto	16° 30′ S	68° 11′ W	4050	*P*, *T*, *V*, *R*, and Ws
Oruro	17° 58′ S	67° 07′ W	3706	*P*, *T*, *V*, *R*, and Ws
Cochabamba	17° 23′ S	66° 10′ W	2570	*P*, *T*, *V*, and *R*
Sucre	19° 03′ S	65° 10′ W	2850	*P*, *T*, *V*, and *R*

Appendix B

A list of Tibetan stations for July 1979 used in the derivation of $T_g - T_a$ regression equation.

Stations	Latitude	Longitude	Elevation
Chengdu	30° 40′ N	104° 01′ E	508
Lhasa	29° 42′ N	91° 08′ E	3659
Xichang	27° 53′ N	102° 18′ E	1592
Kunming	25° 01 N	102° 41′ E	1892
Hekou	22° 30′ N	103° 57′ E	138
Oamdo	31° 11′ N	96° 59′ E	3242

References

Arking, A. and Vemury, S.: 1984, 'The Nimbus 7 ERB Data Set: A Critical Analysis', *J. Geophys. Res.* **89**, 5071–5089.

Brichambaut, P. de: 1975, '*Cahiers A.F.E.D.E.S.*', Supplement au no 1. Editions Europeaennes Thermique et Industrie, Paris.

Chen, L. X., Gong, Z. B., Wang, Z. X., and Chen, J. B.: 1965, 'The Budget of Atmospheric Radiation Energy (III)', *Acta. Meteor. Sinica* **3591**, 6–17.

Chen, L., Reiter, E. R., and Feng, Z.: 1985, 'The Atmospheric Heat Source Over the Tibetan Plateau May–August 1979', *Mon. Wea. Rev.* **113**, 1771–1790.

Cooper, P. I.: 1969, 'The Absorption of Solar Radiation in Solar Stills', *Sol. Energy* **12**, 333–346.

Cressman, G. P.: 1960, 'Improved Terrain Effects of Barotropic Forecast', *Mon. Wea. Rev.* **88**, 327–342.

Flohn, H.: 1968, '*Contribution to a Meteorology of the Tibetan Highlands*', *Atmos. Sci.* Paper No. 130. Colorado State University, Department of Atmospheric Science, Fort Collins, CO 80523.

Gates, W. L. and Nelson, A. B.: 1973, '*A New Tabulation of the Scrips Topography on a 1° Global*', *Part 1. Terrain Heights*. Defense Advanced Project Agency R-1276-ARPA.

Glover, J. and McCulloch, J. S. G.: 1958, 'The Empirical Relation Between Solar Radiation and Hours of Sunshine', *Q.J.R. Meteorol. Soc.* **84**, 172–175.

Gutman, G. J. and Schwerdtfeger, W.: 1965, 'The Role of Latent and Sensible Heat for the Development of a High Pressure System Over the subtropical Andes in the Summer', *Meteorologische Rundschau*. **18** Jahrgang, 3, Heft seite 69–75.

Hahn, D. G. and Manabe, S.: 1975, 'The Role of Mountains in South Asia Monsoon Circulation', *J. Atmos. Sci.* **32**, 1515–1541.

Iqbal, M.: 1983, '*An Introduction to Solar Radiation*', Academic Press, New York, 390 pp.
Kondratyev, K. Ya: 1972, '*Radiation Processes in the Atmosphere*', Second IMO lecture, W.M.O., No. 309.
Krishnamurti, T. N., Daggupaty, S. M., Fein, J., Kanamitsu M., and Lee, J.: 1973, 'Tibetan High and Upper Tropospheric Circulation During Northern Summer', *Bull. Amer. Meteorol. Soc.* **54**, 1234–1250.
Kuo, H. L. and Qian, Y. F.: 1981, 'Influence of the Tibetan Plateau on Cumulative and Diurnal Changes of Weather and Climate in Summer', *Mon. Wea. Rev.* **109**, 2337–2356.
Kuo, H. L. and Qian, Y. F.: 1982, 'Numerical Simulation of the Development of Mean Monsoon Circulation in July', *Mon. Wea. Rev.* **110**, 1879–1897.
Landsberg, H. E., Lippmann, H., Paffen, K. H., and Troll, C.: 1963, *World Maps of Climatology*', Springer-Verlag, Berlin–Gottingen–Heidelberg.
Luo, H. and Yanai, M.: 1983, 'The Large-Scale Circulation and Heat Sources Over the Tibetan Plateau and Surrounding Areas During the Early Summer of 1979, Part I: Precipitation and Kinematic Analyses', *Mon. Wea. Rev.* **111**, 922–944.
Luo, H. and Yanai, M.: 1984, 'The Large-Scale Circulation and Heat Sources Over the Tibetan Plateau and Surrounding Areas During the Early Summer of 1979. Part II: Heat and Moisture Budgets', *Mon. Wea. Rev.* **112**, 966–989.
Matthews, E.: 1983, 'Global Vegetation and Land Use: New High Resolution Data Bases for Climate Studies', *J. Clim. Appl. Meteorol.* **22**, 474–486.
Nitta, T.: 1983, 'Observational Study of Heat Sources Over the Eastern Tibetan Plateau During the Summer Monsoon', *J. Meteorol. Soc. Japan* **61**, 590–605.
Rao, G. V. and Boogaard, H. van de.: 1986, '*A Comparison Between the Bolivian and Tibetan Upper Anticyclones*', preprints, Second Conference on Southern Hemisphere Meteorology, Dec. 1–6, 1986, Amer. Met. Soc., Boston, MA.
Reiter, E. R. and Gao, D. Y.: 1982, 'Heating of the Tibetan Plateau and Movements of the South Asian High during Spring', *Mon. Wea. Rev.* **110**, 1694–1711.
Schwerdtfeger, W.: 1961, 'Stromungs- und Temperaturfeld der Freien Atmosphare über den Anden', *Meteorologische Rundschau* **14**, 1.
Schwerdtfeger, W.: 1976, 'Climates of Central and South America', *World Survey of Climatology*, vol. XII, Elsevier, 532 pp.
Shaeffer, J. D. and Reiter, E. R.: 1987, 'Measurements of Surface Energy Budget in the Rocky Mountains of Colorado', *J. Geophys. Res.* **92**, 4145–4162.
Shen, R., Reiter, E. R., and Bresch, J. F.: 1986, 'Some Aspects of the Effects of Sensible Heating on the Development Summer Weather Systems Over the Tibetan Plateau', *J. Atmos. Sci.* **43**, 2241–2260.
Smith, E. A. and Reiter, E. R.: 1986, 'Monitoring the Spring–Summer Surface Energy Budget Transition in the Gobi Desert Using AVHRR GAC Data', Second Conference on Satellite Meteorology, May 13–16, 1986. Amer. Meteorol. Soc., Boston, MA.
Spencer, J. W.: 1971, 'Fourier Series Representation of the Position of the Sun', *Search* **2**, 172.
Staff Members, Section of Synoptic and Dyn. Meteor., Inst. of Geophys. and Meteor. Academia Sinica, 1958: On the general circulation over eastern Asia II. *Tellus* **10**, 299–312.
United States Department of Commerce: 1979a, 'Monthly Climatic Data for the World', Available from the National Climate Center, Federal Building, Asheville, NC 28801.
United States Department of Commerce: 1979b, 'Environmental Satellite Imaginary, January, 1979', Available from the National Technical Information Service (NT IS), U.S. Dept. of Commerce, Sills Building, 5285 Port Royal Road, Springfield, VA 22161.
van de Boogaard, H., Rao, G. V., and Joseph, D.: 1989, 'The Mean Circulation of the Tropical and Subtropical Atmosphere, January', Scheduled for Publications in 1989 by the National Center for Atmospheric Research, Boulder, Colorado.
Virji, H.: 1981, 'A Preliminary Study of Summer Time Tropospheric Winds', *Mon. Wea. Rev.* **109**, 599–610.
Yeh, T. C. and Chang, C. C.: 1974, 'A Preliminary Experimental Simulation on the Heating Effect of the Tibetan Plateau and the General Circulation Over Eastern Asia in Summer', *Sci. Sin.* **17**, 397–40.

Yeh, T. C. and Gao, Y. X.: 1979, '*The Meteorology of the Qinghai-Xizang Plateau*', Science Press, Beijing, 278 pp. (in Chinese).
Zheng, Q. and Liou, K. N.: 1986, 'Dynamic and Thermodynamic Influences of the Tibetan Plateau on the Atmosphere in a General Circulation Model', *J. Atmos. Sci.* **43**, 1340–1354.